

# Electrical control of parametric processes in silicon waveguides

Kevin K. Tsia, Sasan Fathpour, and Bahram Jalali

*Optoelectronic Circuits and Systems Laboratory  
Electrical Engineering Department  
University of California, Los Angeles, CA, 90095 USA  
[tsia@ee.ucla.edu](mailto:tsia@ee.ucla.edu), [sasan@ee.ucla.edu](mailto:sasan@ee.ucla.edu), [jalali@ucla.edu](mailto:jalali@ucla.edu)*

<http://www.ee.ucla.edu/~oecs/>

**Abstract:** We demonstrate electrical tuning of phase mismatch in silicon wavelength converters. Active control of birefringence induced by a thin-film piezoelectric transducer integrated on top of the waveguides is used for dispersion engineering. The technology provides a solution for compensating the phase mismatch caused by fabrication errors in integrated waveguides. It also offers a mean to dynamically control the relative dispersion between interacting waves and hence, to introduce electronic control of optical parametric processes.

©2008 Optical Society of America

**OCIS codes:** (130.4310) Integrated optics, nonlinear; (190.4390) Nonlinear optics : Nonlinear optics, integrated optics; (190.4975) Parametric processes.

---

## References and links

1. B. Jalali, "Teaching silicon new tricks," *Nature Photonics*, **1**, 193-195, (2007).
2. Q. Lin, O. J. Painter, and G. P. Agrawal, "Nonlinear optical phenomena in silicon waveguides: modeling and applications," *Opt. Express* **15**, 16604-16644 (2007).
3. M. A. Foster, A. C. Turner, J. E. Sharping, B. S. Schmidt, M. Lipson, A. L. Gaeta, "Broad-band optical parametric gain on a silicon photonic chip," *Nature* **441**, 960-962 (2006).
4. M. A. Foster, A. C. Turner, R. Salem, M. Lipson, and A. L. Gaeta, "Broad-band continuous-wave parametric wavelength conversion in silicon nanowaveguides," *Opt. Express* **15**, 12949-12958 (2007).
5. D. Dimitropoulos, V. Raghunathan, R. Claps, and B. Jalali, "Phase-matching and nonlinear optical processes in silicon waveguides," *Opt. Express* **12**, 149-160 (2004).
6. V. Raghunathan, R. Claps, D. Dimitropoulos, B. Jalali, "Parametric Raman wavelength conversion in scaled silicon waveguides," *J. Lightwave Technol.* **23**, 2094-2102 (2005).
7. W. N. Ye, D. -X. Xu, S. Janz, P. Cheben, M. -J. Picard, B. Lamontagne, and N. G. Tarr, "Birefringence control using stress engineering in silicon-on-insulator (SOI) waveguides," *J. Lightwave Technol.* **23**, 1308-1317 (2005).
8. V. Raghunathan, and B. Jalali, "Stress-induced phase matching in silicon waveguides," *Conference of Lasers and Electro-Optics (CLEO), Long Beach CA (2006) Paper CMK5*.
9. K. K. Tsia, S. Fathpour, and B. Jalali, "Electrical tuning of birefringence in silicon waveguides," *Appl. Phys. Lett.* **92**, 061109 (2008).
10. N. Setter, *Electroceramic-based MEMS: fabrication-technology and applications* (Springer, New York 2005).
11. H. Ishiwara, M. Okuyama, and Y. Arimoto, *Ferroelectric random access memories: fundamentals and applications* (Springer, New York, 2004).
12. K. K. Tsia, S. Fathpour, and B. Jalali, "Energy harvesting in silicon wavelength converters," *Opt. Express* **14**, 12327-12333 (2006).
13. G. P. Agrawal, *Nonlinear Fiber Optics*, 4th ed. (Academic Press, Boston, 2007)

## 1. Introduction

Silicon photonics has made spectacular progress in the last few years. Particularly, strong third-order optical nonlinearity in silicon has led to a wide range of functionalities that were believed to be absent in silicon [1,2]. Among them are wavelength converters, parametric amplifiers and oscillators. Such devices are based on either four-wave mixing (FWM) using the Kerr effect, or coherent anti-Stokes Raman scattering (CARS). The latter is a form of FWM mediated by the Raman effect. For successful operation, these devices require dispersion engineering because dispersion-induced phase mismatch lowers the efficiency of power transfer between the interacting waves.

A number of techniques for achieving phase-matching in silicon waveguides have been demonstrated. One approach relies on engineering the group-velocity dispersion (GVD) by proper waveguide geometry design to balance the nonlinear phase mismatch. Although this technique allows optical parametric amplification and efficient wavelength conversion, it demands precise control of waveguide dimensions (<50 nm) [3,4] in order to achieve the prerequisite dispersion, placing stringent requirements on fabrication tolerances.

Another approach is to use modal birefringence of the interacting waves to compensate the chromatic dispersion [5,6]. Birefringence control can be achieved by control of waveguide dimensions, which is, again, subjected to fabrication errors. However, birefringence can also be tuned by applying stress to the waveguide [7,8]. Direct application of mechanical stress via a load-cell has been reported for dynamic phase-matching in CARS wavelength conversion through stress-induced birefringence [8]. Clearly, using an external load-cell is not a practical solution for integrated optics. Integration of a piezoelectric layer onto silicon photonics platform solves this predicament. We recently demonstrated electrical tuning of birefringence in silicon-on-insulator (SOI) waveguides by the stress induced by a thin-film piezoelectric transducer integrated on top of the waveguide [9]. In this paper, we demonstrate active tuning of phase-matching in SOI-waveguide wavelength converters. Specifically, the birefringence induced by a piezoelectric transducer is used to actively control the phase-matching of wavelength conversion via CARS. This technology ensures phase matching even in the presence of fabrication-induced uncertainties in waveguide dimensions. It can also be used within a feedback loop to maintain phase matching in the face of environmental induced variations. We note that varying the stress in the waveguide alters the dispersion for cross-polarized beams. Hence, this technology can be useful for GVD engineering.

## 2. Working principles

The device structure consists of a SOI rib waveguide with a top oxide-cladding layer, on top of which a thin film piezoelectric capacitor is formed (Fig. 1). Among the various piezoelectric materials, lead zirconate titanate (PZT) was chosen because of its strong piezoelectric effect. PZT is the most commonly used piezoelectric material and appears in ultrasonic transducers, micro-electro-mechanical (MEMS) devices and ferroelectric random-access memories [10,11]. Our PZT transducer consists of a thin film PZT layer sandwiched between a top and a bottom platinum/titanium (Pt/Ti) electrode. The oxide top cladding is required to minimize the optical absorption loss resulting from the bottom electrode. The geometrical dimensions of the structure are described in caption to Fig. 1. Optical simulations based on the BeamProp software confirms that the present waveguide structure is single-mode and the induced stress, notwithstanding the existence of the PZT capacitor overlaid layer, does not alter its optical properties as compared with devices without the capacitor. More details on the fabrication and PZT film properties were reported in a previous publication [9].

By applying voltage across the PZT capacitor, the piezoelectric effect in PZT induces the anisotropic stress, or equivalently strain. It results in breaking the centrosymmetry of the silicon crystal and leading to material birefringence in silicon as governed by photoelastic effect. We propose and demonstrate the use of this tunable birefringence effect for active phase matching in silicon waveguides.

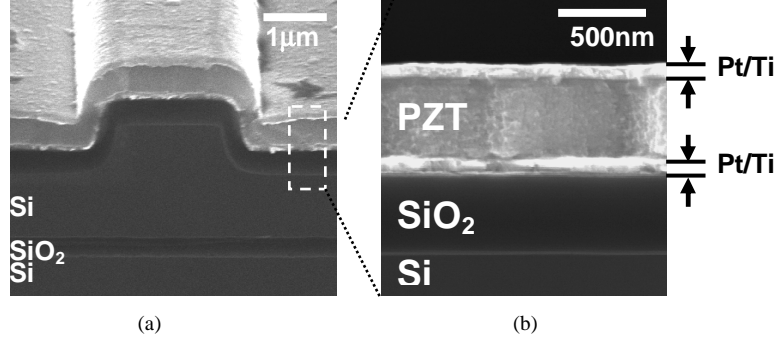


Fig. 1 (a) Scanning electron microscope image of the SOI waveguide with the PZT capacitor on top of it. (b) The enlarged cross-section of the PZT capacitor. The waveguide has a width of 1.5  $\mu\text{m}$ , rib height of 2  $\mu\text{m}$  and slab height 1.1  $\mu\text{m}$ . The oxide-cladding is 500 nm thick. The PZT thickness is 500 nm. Both top and bottom Pt/Ti electrodes are 100nm/10nm thick.

Efficient CARS wavelength conversion in silicon waveguides requires phase-matching among Stokes, anti-Stokes and pump waves, which span  $\sim 200$  nm in wavelength at near infrared [6]. The phase matching condition for the CARS process is:

$$k_A^j = 2k_P^i - k_S^j, \quad (1)$$

where  $k_P$ ,  $k_S$  and  $k_A$  are the propagation constant at pump, Stokes and anti-Stokes wavelength, respectively. The superscripts  $i$  and  $j$  refer to transverse electric (TE) or transverse magnetic (TM) polarizations. Deviations from phase matching can be expressed as  $\Delta k = 2\Delta k_B + \Delta k_{WG} + \Delta k_{MAT}$ , where  $\Delta k_B$  is the phase mismatch due to modal birefringence at pump wavelength, defined as the difference between the effective indices of TE,  $n_{TE}$ , and TM,  $n_{TM}$ , waveguide modes,  $\Delta k_{WG}$  is the chromatic dispersion associated with wavelength dependence of modal area, and  $\Delta k_{MAT}$  is due to material dispersion. The waveguide considered in this paper operates in normal dispersion regime. The phase mismatch due to waveguide and material dispersion, i.e.,  $\Delta k_{WG} + \Delta k_{MAT}$ , is in the order of  $-100 \text{ cm}^{-1}$  [5,6]. Birefringence phase mismatch,  $\Delta k_B$ , can be used to compensate  $\Delta k_{WG}$  and  $\Delta k_{MAT}$ , and consequently phase matching condition can be attained. Note that we neglect the nonlinear phase-mismatch in Eq. (1) as it has negligible effect on the overall phase-matching condition for the present waveguide design [6].

In the context of the present work, two main components contribute to  $\Delta k_B$ . The first component is the static birefringence,  $\Delta n_{B0}$ , due to the asymmetric geometry of the rib waveguide and the material birefringence induced by the residual stress of the cladding layers that cover the rib. The second component is the tunable birefringence due to the stress induced by the PZT,  $\Delta n_{piezo}$ . This is related to the difference of stress in horizontal and vertical directions in the waveguide, Young's modulus, Poisson's ratio and the photoelastic tensor elements of silicon [9]. As such,  $\Delta k_B$  can be expressed as

$$\Delta k_B = \frac{2\pi}{\lambda_p} (n_{TE} - n_{TM}) = \frac{2\pi}{\lambda_p} (\Delta n_{B0} + \Delta n_{piezo}) = \Delta k_{B0} + \Delta k_{piezo}, \quad (2)$$

where  $\Delta k_{B0} = 2\pi\Delta n_{B0}/\lambda_p$  and  $\Delta k_{piezo} = 2\pi\Delta n_{piezo}/\lambda_p$  are phase mismatches corresponding to the static birefringence and the tunable birefringence, respectively, and  $\lambda_p$  is the pump wavelength. It should be emphasized that the role of  $\Delta k_{piezo}$  is to provide additional degree of freedom to fine-tune the phase mismatch arising from fabrication-induced errors, such as uncertainties in waveguide dimension and the stress of the cladding layers.

### 3. Experiments and results

The Fabry-Pérot (FP) resonance technique was used to measure the waveguide loss and the material birefringence induced by piezoelectricity  $\Delta n_{piezo}$ , from which,  $\Delta k_{piezo}$  can be calculated. The 2-cm long silicon waveguide integrated with the PZT capacitor exhibits low

linear propagation loss of 0.6 dB/cm, a value that is virtually the same as that measured before the addition of the PZT and its metal electrodes. It suggests that the upper waveguide cladding layer is effective in isolating the optical mode from the lower PZT electrode. Varying the PZT voltage from  $-10$  V to  $5$  V, the overall birefringence tuning range was measured to be  $\Delta n_{\text{piezo}} \approx 1 \times 10^{-4}$ , which leads to  $\Delta k_{\text{piezo}} \approx 4 \text{ cm}^{-1}$  (Fig. 2). We note that the birefringence tuning range reported here is  $\sim 3$  times higher than the value reported in ref. [9]. The sensitivity of birefringence on waveguide dimensions was quantified in ref. [5]. Based on that work [5], our measured birefringence tuning value of  $\Delta n_{\text{piezo}} \approx 1 \times 10^{-4}$  is sufficient to compensate the phase-mismatch caused by up to  $\sim 50$  nm in fabrication induced errors in waveguide dimension.

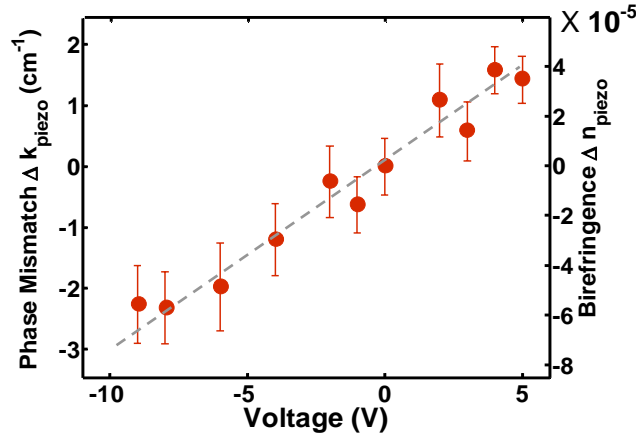


Fig. 2 Phase mismatch (left axis) and the corresponding birefringence (right axis) of the SOI waveguide due to piezoelectric effect from PZT as a function of DC voltages.

In the CARS wavelength conversion experiment, the pump beam is from an external cavity diode laser, amplified by an Erbium-doped fiber amplifier at 1538 nm (TE polarized). The Stokes signal is from a distributed feedback (DFB) fiber laser at 1673 nm (TM polarized). The pump and Stokes are combined by a wavelength division multiplexer (WDM) and coupled into and out of the waveguide by two identical objective lenses (NA = 0.40). The polarization states of the pump and Stokes signals are controlled by the polarization controllers before the WDM. The output light from the waveguide is sent to an optical spectrum analyzer (OSA). The polarization state of the converted anti-Stokes signal at 1424 nm (TM-polarized) is verified by an analyzer before the OSA.

Figure 3(a) and (b) show the measured anti-Stokes spectra at different bias voltages applied across the PZT capacitor, under two different input polarization conditions. The coupled input pump power is  $\sim 1.2$  W. Conversion efficiency is defined as the ratio of the Stokes signal to the anti-Stokes signal at the waveguide output [3,4]. We note that both Stokes and anti-Stokes suffer from free-carrier absorption (FCA) loss. By comparing the Stokes power at the output for pump-on (1.2 W) and pump-off states, we measure an on-off loss of  $\sim 1$  dB for the Stokes signal. Assuming both Stokes and anti-Stokes signals travel the same distance through the waveguide, the anti-Stokes loss will be about 30% lower due to the wavelength dependence of FCA [2].

By varying the DC bias applied to the PZT capacitor from 0 V to 5 V, we attain improvement of  $\sim 6$  dB in conversion efficiency (Fig. 3(a)). Enhancement in efficiency only occurs when the pump and the Stokes are cross-polarized (Fig. 3(a)) as compared with the co-polarized case (Fig. 3(b)). This verifies that the effect originates from the birefringence induced by the PZT capacitor. The 0.2-0.3nm 3dB-bandwidth of the anti-Stokes signal in Fig. 3 is limited by the OSA. A low resolution setting was used in order to maximize the measurement throughput.

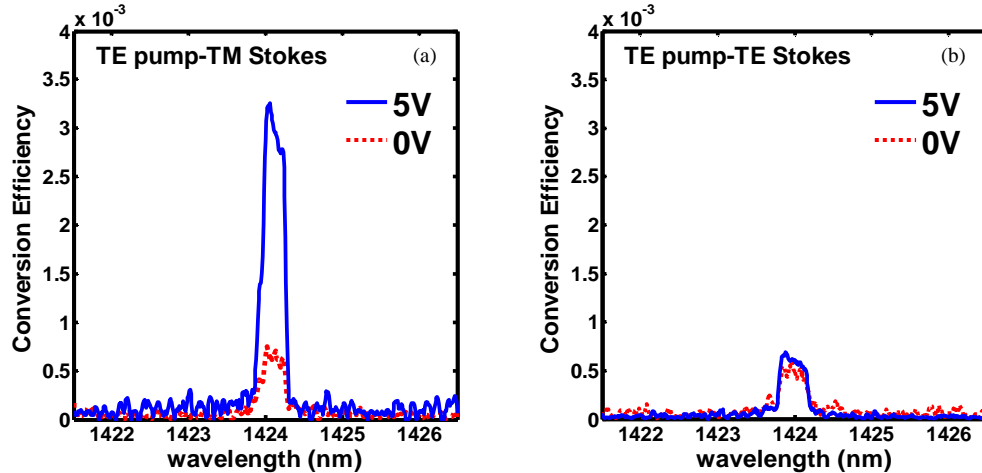


Fig. 3 Anti-Stokes spectra (TM polarized) of wavelength conversion based upon coherent anti-Stokes Raman scattering at voltage biases of 0V (red) and 5V (blue) applied to the PZT capacitor. Two input conditions are studied: (a) TE-polarized pump and TM-polarized Stokes. (b) TE-polarized pump and TE-polarized Stokes. The coupled input pump power is  $\sim 1.2$  W.

Figure 4(a) shows the measured conversion efficiency as a function of the applied voltage. The plot clearly exhibits the hallmark of FWM based conversion efficiency: an oscillatory variation with phase mismatch. In particular, we note that the oscillation depth in conversion efficiency is as high as  $\sim 20$  dB. Based on the coupled-mode analysis of CARS wavelength conversion [5], we calculate the dependence of conversion efficiency on phase mismatch (the red curve in Fig. 4(b)). The simulation uses a Raman gain coefficient of 20 cm/GW [6] and a lifetime of 20 ns. The lifetime value is close to the measured value of 15 ns we have reported previously for similar waveguides [12]. We observed that the oscillatory variation agrees well with the  $\text{sinc}^2$  dependence of the conversion efficiency on phase mismatch [13] (Fig. 4(b)). The figure suggests that these devices achieve a phase-mismatch tuning range of  $5 \text{ cm}^{-1}$  (from  $-15 \text{ cm}^{-1}$  to  $-10 \text{ cm}^{-1}$ ). This value agrees well with direct birefringence measurements shown in Fig. 2. The tunability range reported here is limited by the voltage that could be applied (15 V) before breakdown occurred. Higher tuning range can be achieved by improving the film quality such that it can withstand higher voltages. Also, structural optimization using a finite-element analysis package such as ANSYS [9] may also lead to larger tuning range. Nevertheless, it is important to note that the tuning range of  $5 \text{ cm}^{-1}$  is adequate for compensating for phase mismatches caused by fabrication induced errors in waveguide dimensions.

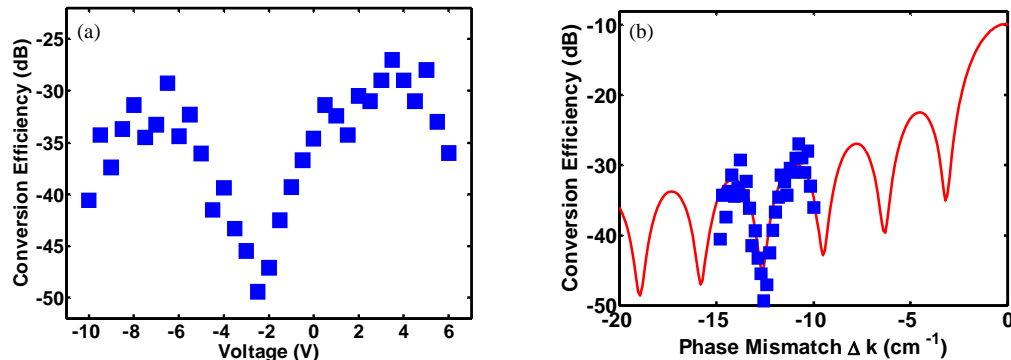


Fig. 4 (a) Measured CARS wavelength conversion efficiency versus PZT voltages at coupled pump power of  $\sim 1.2$  W. (b) Calculated dependence of CARS conversion efficiency on phase mismatch (red curve). The measured data (blue square dots) is fit with the model.

In Fig. 5, the conversion efficiency is plotted versus coupled pump power for two different PZT biases. The plot also shows the conversion efficiency of an air-clad waveguide, i.e., a bare SOI waveguide before depositing the cladding layers. The air-clad waveguide has the lowest efficiency, as it is farthest away from the phase matching condition (grey triangles). The residual stresses of the cladding layers (i.e., oxide, electrodes, and unbiased PZT) introduce a birefringence component that improves the efficiency by 7-8 dB (blue squares). An additional tunable stress can be applied by biasing the PZT, by which a further 5-6 dB enhancement of efficiency can be achieved (red circles). Hence a total improvement of 12-14dB is obtained by the addition of the PZT capacitor. The calculations based on the aforementioned model also match with experimental results at 0 V and 5 V (blue and red curves), which correspond to phase mismatches of  $-12 \text{ cm}^{-1}$  and  $-10.5 \text{ cm}^{-1}$ , respectively.

It is evident from Fig. 4(b) that the dimensions of the present waveguide render it far from phase matching condition (to the phase-mismatch of  $\sim 12 \text{ cm}^{-1}$  at zero bias). While the tunable phase match control, provided by the piezoelectric transducer, is sufficient to compensate for fabrication induced error in waveguide dimensions, it is not enough to bring the waveguide to the zero phase mismatch condition. To arrive at phase matching, one must engineer the waveguide dimensions such that it is closer the phase matching condition. The piezoelectric technology can then correct for the fabrication errors and also to maintain the phase matching condition in the presence of temperature or acoustic induced fluctuations.

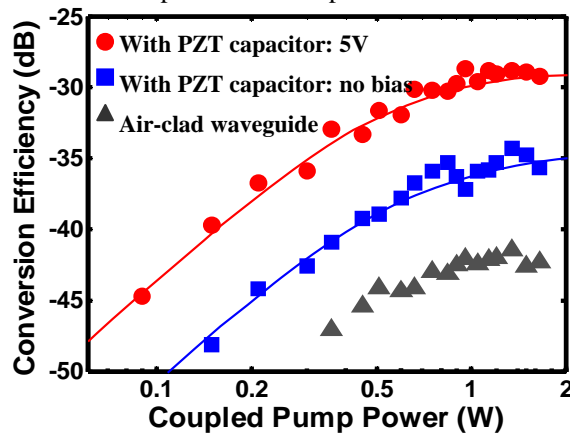


Fig. 5 CARS wavelength conversion versus coupled pump power for air-clad SOI waveguide (grey triangles), the waveguide with PZT capacitor cladding without voltage bias (blue squares) and at a bias of 5 V (red circles). The theoretical model agrees well with the case of 0 V (blue line:  $\Delta k=12 \text{ cm}^{-1}$ ) and 5 V (red line:  $\Delta k=10.5 \text{ cm}^{-1}$ ).

#### 4. Conclusions

We have reported proof-of-principle results on active dispersion control in silicon waveguides. The demonstration was performed in the context of CARS wavelength conversion, a FWM process mediated by the Raman effect. The stress induced by the PZT capacitor introduces an electrically tunable birefringence which can compensate the phase mismatch due to chromatic dispersion among the interacting waves. While phase matching can, in principle, be achieved in a waveguide with a particular cross sectional dimensions, this approach is intolerant to inaccuracies in device fabrication. The technique demonstrated here can correct this and render the device tolerant to fabrication errors. It also provides a mean to dynamically control the relative dispersion between interacting waves and hence, to introduce electronic control of optical parametric processes.

#### Acknowledgement

This work was funded by DARPA under the EPIC program. The authors are grateful to Dr. Jag Shah of DARPA for his support.